Characterization of the level fluctuations in a physical model of the steel continuous casting mold through image processing

J.R. Miranda-Tello, F. Sánchez-Rangel, C.A. Real-Ramírez, G. Khatchatourov, J.A. Aragón-Lezama, L.F. Hoyos-Reyes, E.A. Andrade-González, and J.I. González-Trejo
División de Ciencias Básicas e Ingeniería, Universidad Autónoma Metropolitana-Azcapotzalco, Av. San Pablo 180, Col. Reynosa-Tamaulipas, Del. Azcapotzalco, 02200, México, D.F., México, e-mail: jrmt@correo.azc.uam.mx

Recibido el 13 de diciembre de 2011; aceptado el 24 de enero de 2012

In this work is characterized the periodic behavior of the liquid level inside a scaled cold-model of the mold section of a steel continuous casting machine, which uses water as working fluid. The models are designed in order to simulate the dynamic forces acting on the molten steel inside a mold of continuous casting. The force magnitude can induce choppy flow, waves and vortex formation in the mold. The experimental model uses a closed-loop hydraulic configuration. In the mold, the inlet and the outlet water flow rates are the same. This configuration resembles a perfect control of the liquid level inside the water model. A high-speed video camera was used to get several video clips of the movement of the water level profile. Several techniques were tested in order to obtain the best lighting conditions for recording the water movement. The edge-detection technique of Sobel was used to determine the profile of the liquid level in each one of the images recorded. The analysis of the dynamic behavior of the water profile showed that the fluctuations of the liquid level inside the mold have a complex structure, which is repeated over large time periods.

Keywords: Continuous casting; edge-detection; level control.

PACS: 61.25.Mv; 47.27.E; 42.30.Tz

1. Introduction

Most of the steel produced in the world is obtained through the continuous casting of molten metal. The modern steel industry must reach high standards in steel semi-finished products. It has been reported in the literature that the steel quality depends on the fluid flow phenomena taking place inside the mold of the casting machine [1-2].

Therefore, a good control of the level fluctuations of the molten metal in the continuous casting mold is important to satisfy the specifications of the steel products [3-7]. In the continuous casting of steel, the fluid flow pattern inside the mold produces significant deformations of the liquid free surface; consequently, it is difficult to obtain accurate measurements of the liquid level.

Many experimental investigations have studied the transient variations of the molten steel free surface [8-15]. In literature the dynamic behavior of the liquid height is commonly assumed as a standing wave. Using a scaled model, Miranda *et al*. [8] found that liquid surface fluctuations form complex structures with periodic components.

Shen *et al*. [9-10,16] studied the instability of the liquid free surface in a full-scaled mold of a thin slab continuous casting machine. In their experiments, they used the particle image velocimetry (PIV) technique. Those authors found that level heights and the location of the centers of the recirculation zones, have a cyclic behavior and the characteristic periods are similar to that reported by Miranda *et al*. [8]. It was also found that the wave height depends on the jet depth and the position of the recirculation zones.

Jeon *et al*. [11] investigated the fluid flow pattern oscillation and the fluctuations of the meniscus in two funnel-type molds with three types of submerged entry nozzles (SEN). They employed PIV measurements to characterize the flow pattern inside the mold. In that work, images recorded with a video camera were used to obtain the meniscus levels by applying an edge-detection technique. Due to the low frequency at which video clips were recorded, they obtained blurred images. In addition, shadows were recorded because of the poor lighting conditions. Nevertheless, those images were used in order to determining the level profile.

Yuan *et al*. [12] quantified some characteristics of the transitory behavior of the fluid flow in a continuous casting mold by using PIV measurements. They compared experimental results against numerical simulations. The turbulence model employed in the mathematical model was the large eddy simulation (LES). They found a complex structure of the vortexes, which are evolving and reconstructing in both, the upper and lower recirculation zones. Real *et al*. [17] describe the underlying phenomena of this behavior and discuss its relationship with the liquid free surface.

Yuan *et al*. [12] also observed that along the time the velocities at the free-surface displays an intermittent behavior. In accordance with these authors, the irregular trajectories of the tracking particles are evidence of chaotic motion.

Gupta *et al*. [14] studied the transitory behavior of the asymmetric fluid flow patterns inside a scaled mold filled with water. Although the recording speed was 25 frames per second, their experiments provided qualitative information about the auto-sustained oscillation of the flow pattern. In a subsequent work, Gupta *et al*. [13] reported that the fluid flow pattern inside the mold is asymmetric, and it oscillates around the central plane with a random time period.

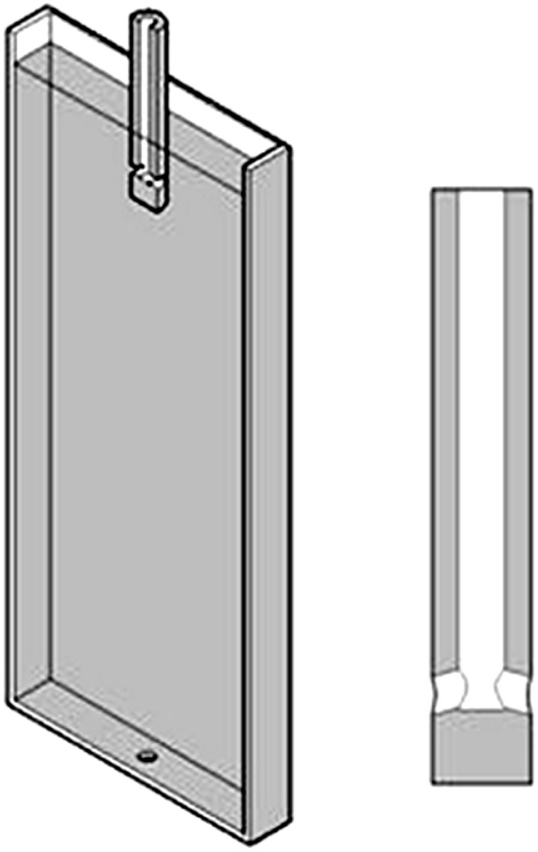

FIGURE 1. Schematic representation of a scaled mold. a) Isometric view of one-half of the mold, b) Internal path geometry of the SEN.

This work uses an image-processing algorithm to measure the liquid level inside a scaled model of the continuous casting mold. This is a non-invasive technique which employs images captured with a high-speed video camera. The algorithm to processing the images used to measure the liquid level was programmed in Matlab. The time series of the level profile along the mold width were analyzed using short and long-time scales to isolate the high and low frequency signal components. The short-time scale analysis showed that there is a periodic component with a characteristic frequency close to that reported in literature. The long-time scale analysis showed a complex component of low frequency, which has not been reported in literature.

2. Static model and images characteristics

Physical models are frequently used in experimental investigations to study the fluid flow phenomena and the behavior of the continuous casting process [16]. These models are designed considering some similarity criteria, and commonly, the water substitutes the molten steel. The aim of these scaled models is to reproduce the hydrodynamic comportment of the molten metal, as well as the fluctuations of the free surface of liquid steel. These phenomena occur in a current mold of steel continuous casting machine.

Figure 1 shows a schematic representation of the physical model used in this work. It has a 1:3 scale ratio, and its dimensions are 1200 mm long, 500 mm width and 87 mm thick. The scaled model is a rectangular prism and is made of acrylic. The water is discharged into the mold by a cylindrical bifurcated pipe, known as the submerged entry nozzle (SEN). The SEN is fixed on the top of the mold. The dimensions of the SEN are 320 mm of length, 53.97 mm of external diameter and 25.4 mm of inner diameter. The SEN has two exit ports with a diameter of 20 mm. Each one has 15 degrees downwards inclination with respect the horizontal (see Fig. 1b). The SEN is situated at the mold centerline.

Figure 2 shows a schematic representation of the experimental setup. At the bottom of the mold is the outlet of the water. The outflow is again introduced into the mold by a centrifugal pump. This configuration ensures that the inlet and outlet flow rates are the same. Therefore, this liquid circuit resembles a perfect control of the liquid level in an industrial facility.

The experimental operating conditions correspond to a nominal casting speed of 1.8 m/min. The water flow rate circulating through the model was measured with a digital flow meter installed in the hydraulic circuit between the mold outlet and the SEN. The SEN submergence depth is the liquid height measured from the center of the SEN exit ports to the free surface when the pump is turned off. The submergence depth of the SEN used in the experiments was 70 mm.

3. Detection of the level profile in the model

Some investigations related to the study of the continuous casting process analyzed the liquid level inside the mold by applying the edge-detection technique to recorded images of the experiments [11,15,18]. The aim of the edge-detection is to produce a set of points that are obtained after identifying

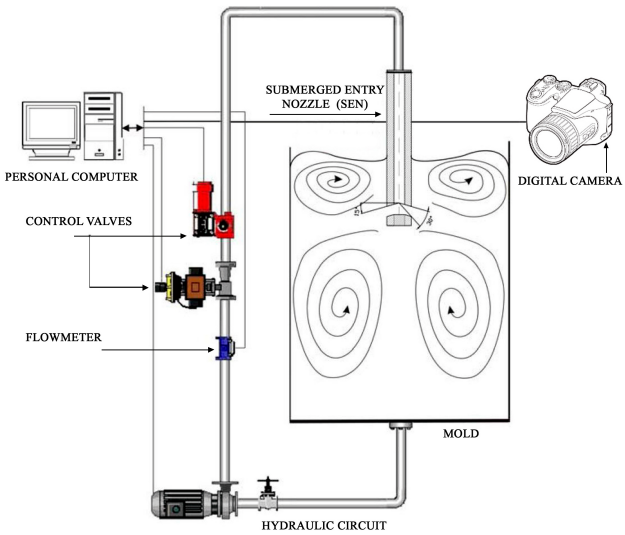

FIGURE 2. Schematic diagram of the experimental setup.

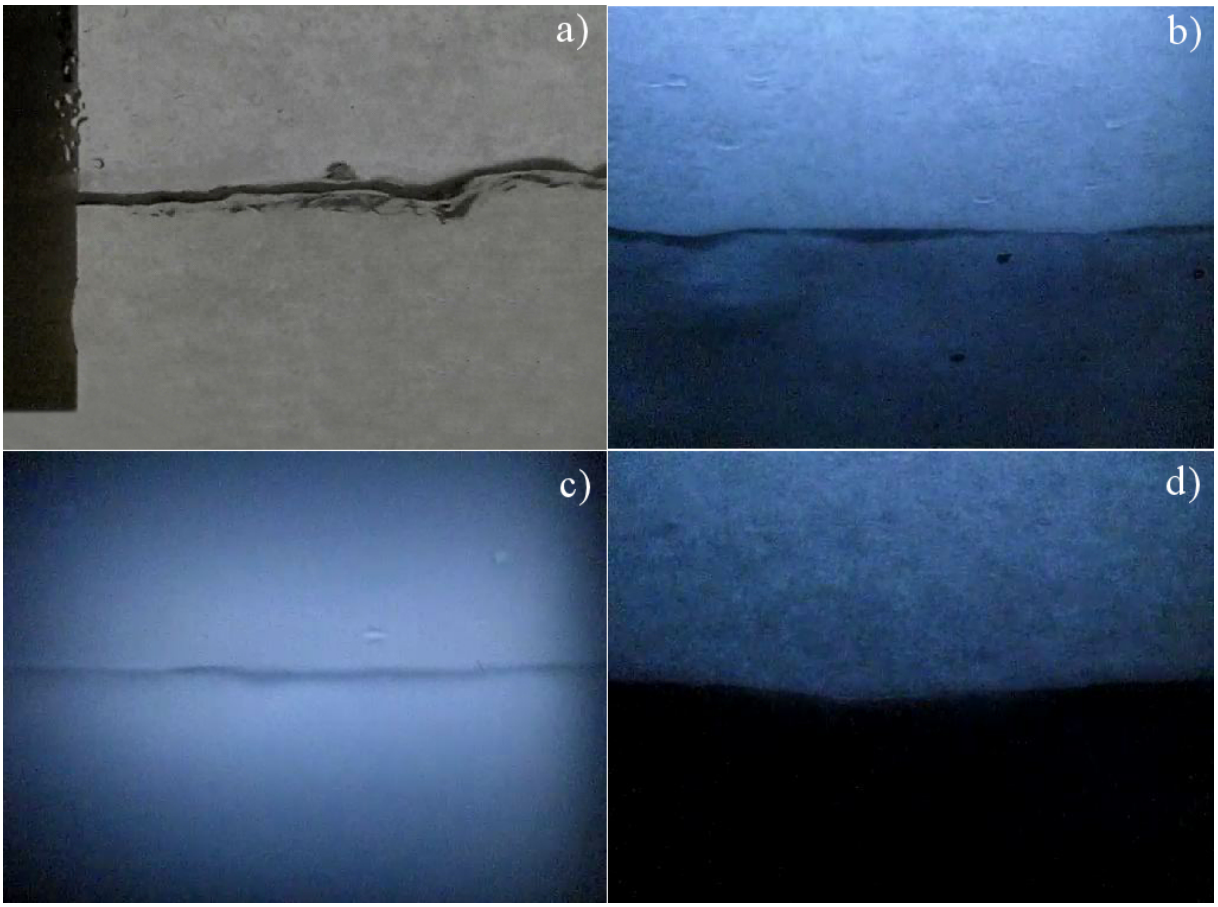

FIGURE 3. Images using different locations of the diffuser and lighting styles.

ing the pixels where the image brightness intensity suddenly changes [18-20].

To accomplish the measurements of the liquid level inside the water model, the edge of the free-surface profile was determined using an image-processing technique. Each of the processed images belongs to a high-speed video clip that records the movement of the level. The recording speed was 300 frames per second at 512×384 pixels of resolution. To obtain higher resolution in measuring the height of the level, was recorded only one-half of the mold.

The quality of the image is a central concern regardless of the method used in the edge-detection [21]. Lighting plays a key role to improve the results of image processing techniques [21-22]. The following strategies were used in the experiments to enhance the contrast of the recorded level profile. The low-key lighting style emphasizes the contours of an object by creating a chiaroscuro effect and only requires one main light. Light reflectors and diffusers are commonly used in photography to homogenize the lighting over the recorded object. A diffuser is any device that scatters light to obtain soft light. The light diffuser can be made with materials like translucent glass, acrylic, opal glass, etc.

Figure 3 shows the effect on the quality of recorded images using several lighting conditions and light diffusers. In these experiments, the camera is located at the same height as the liquid free surface.

Solar lighting was used to record the image shown in Fig. 3a. Artificial lighting was used to record the experiments shown in Figs. 3b, 3c and 3d. The main light is at the top of the mold in Figs. 3b and 3d. In Fig. 3c, the main light is behind the mold, at the same height as the level profile.

A light diffuser was employed in all the images shown in Fig. 3. In Figs. 3a, 3b and 3c, the light diffuser is behind the mold, while in Fig. 3d, the diffuser is at the front of the mold. Figure 3 shows that the best contrast on the images is obtained when a diffuser is located behind the mold, and the main light is at the top of the mold.

In the experiments showed in Fig. 3, the depth of field (DOF) was adjusted to obtain a liquid level profile as sharpened as possible. An accurate measurement of the liquid level cannot be done because the shape of the free surface is not flat and water is translucent. Therefore, the water was colored using white color ink and a black color diffuser behind the mold was used in order to enhance the sharpness of the level profile.

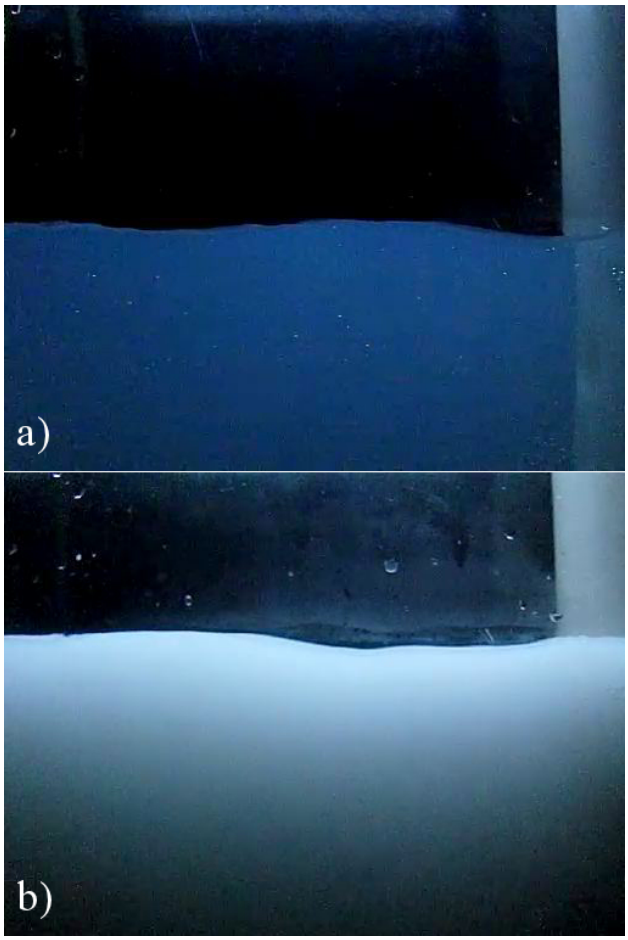

FIGURE 4. Effect of the color intensity in the liquid inside the mold.

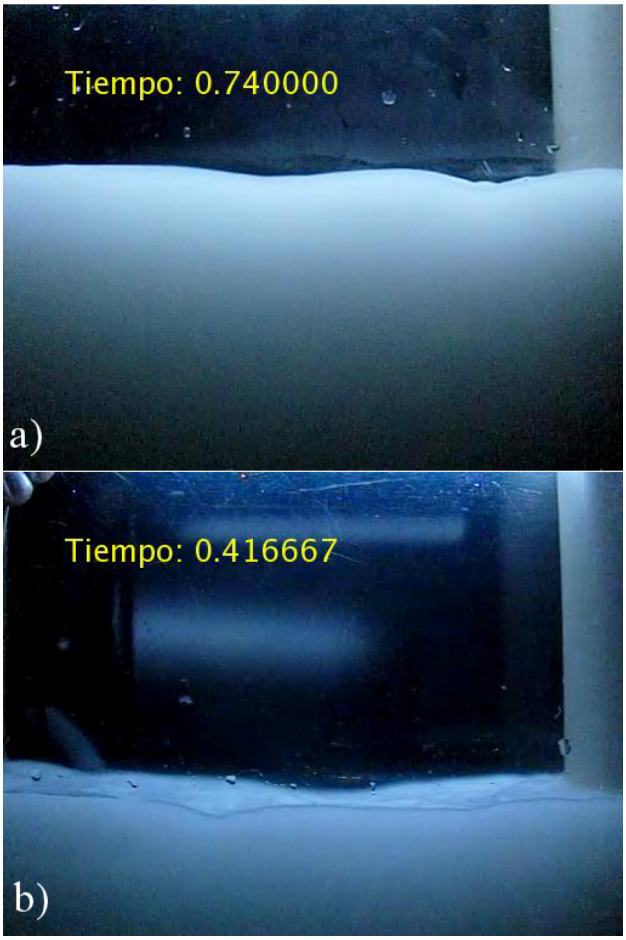

FIGURE 5. Images recorded using different camera heights.

Figure 4 shows the effect of the color intensity of the liquid inside the mold. Figure 4a shows a poorly defined level when the color intensity is low and a distortion of the free surface is obtained. By contrast, the profile of the liquid level is sharpened when the dye concentration is high (Fig. 4b). Therefore, the color intensity used in experiment shown in Fig. 4b was used in the rest of the experimental simulations.

The height of the camera can be adjusted to reducing the reflections produced by the liquid free-surface. Figure 5 shows the effect of the camera height. Figures 5a and 5b show captured images when the camera height is lower and higher than the liquid level respectively. To choose the best location of the camera, an edge-detection technique will be applied to the images shown in Fig. 5.

Color images must be transformed to gray-tones images before applying any edge-detection technique. The edges are the pixels that present a sharp variation in the gray levels [18,20,23].

The objective of any edge-detection technique is to locate only the edges generated by the elements in the scene. Wide variety of edge detectors have been proposed in the literature, including classical methods such as the Prewitt and Sobel algorithms, as well as some algorithms more sophisticated [19].

In the present work, the Sobel-algorithm was used, because of this technique uses two filters in order to detect vertical and horizontal borders [20]. One advantage of this method, is that the quality of the edge detection can be adjusted by changing the threshold value [18].

Figure 6 shows the results obtained by applying the Sobel-method with two different threshold values to the images presented in Fig. 5. A threshold value of 0.02 was used in Figs. 6a and 6b, whereas a value of 0.06 was used in Figs. 6c y 6d. If a small threshold value is employed undesirable details of the picture like shadows are recovered. Figures 6b and 6d show that there exist at least two edges of the liquid free-surface when the camera is located too high. Figure 6c shows that the level profile can be accurately measured when the camera is located slightly higher than the liquid level, and a threshold value is appropriately chosen.

4. Result and discussions

The experiments were carried out using the scaled model, and the bifurcated submerged entry nozzle described previously in Sec. 2. The water flow rate and the SEN submergence depth were 2.28 $m^3\ s^{-1}$ and 70 mm respectively.

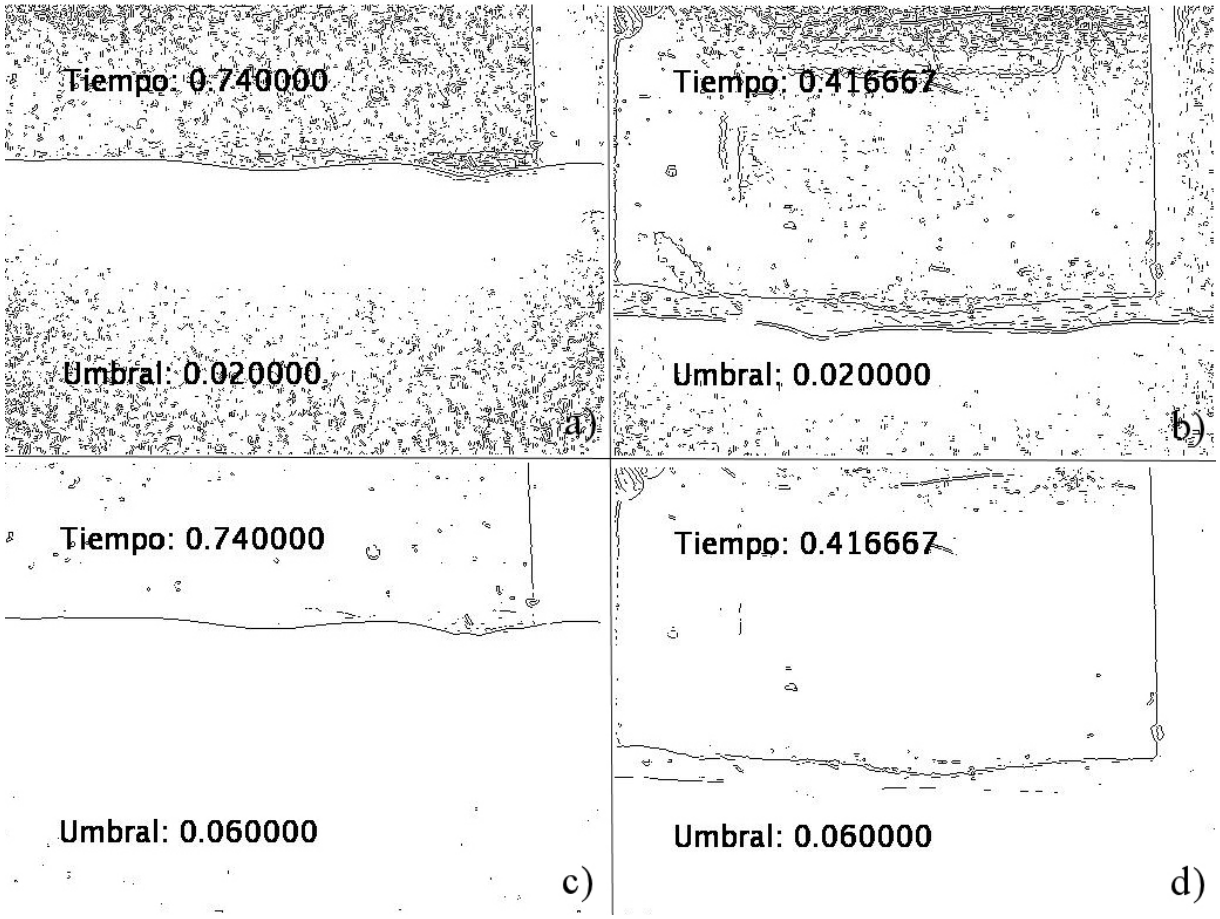

FIGURE 6. Images obtained by edge-detection technique with different values of threshold.

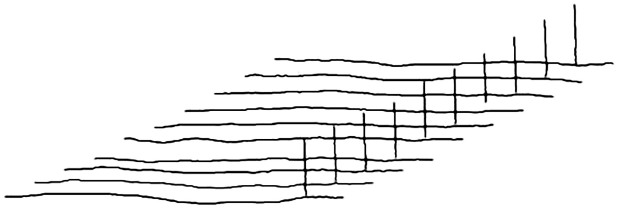

FIGURE 7. Sequence of edges detected using the Sobel technique.

These parameters were chosen in order to reproduce the hydrodynamic behavior of a current steel casting speed of 1.8 m min^{-1}. In all the experiments, the lighting and the camera location were set according to the procedure described earlier, to avoid processing blurred images or with shadows in the meniscus zone.

Several video clips were recorded to characterize the periodic behavior of the free surface height of the water. The extent of the videos was two-minutes long. In all cases, the recording speed was 300 frames per second and image resolution was 512×384 pixels. Therefore, 36,000 images were recorded in each experiment. These images were processed to characterize the dynamic behavior of the free surface profiles. In most reported studies, the experiments were conducted using a recording speed of 30 frames per second, a value ten times slower than the speed used in the present work.

Figure 7 shows several water level profiles obtained from the edge-detection technique. The vertical line belongs to the SEN edge. The time interval between each edge of this figure is 0.1 s. This series of images illustrates the changes of the water level profile along the time.

4.1. Short-time scale

Figure 8 shows the dynamic behavior of the water level height corresponding to a period of two seconds long. The surface was colored in accordance with its height. The edges detected in all the images composing the video were included in this figure. Furthermore, it clearly illustrates the variations in the height of the liquid level along the time.

Figure 8 exhibits a pattern that is repeated five times along an interval of two seconds, which signifies that this pattern has a frequency of approximately 2.5 Hz. In order to validate this, a formal analysis of the power spectral density of the signal must be conducted. This periodic behavior is quite

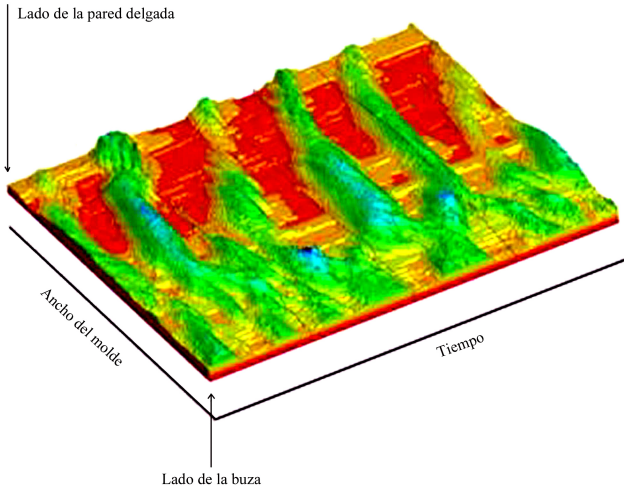

FIGURE 8. Transient behavior of the water level height along a two-seconds clip.

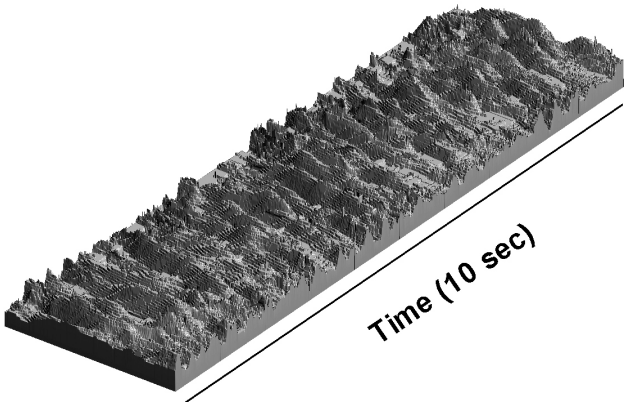

FIGURE 9. Dynamic behavior of the water level profile along a ten-seconds video clip.

evident in the adjacent zone to the narrow-wall of the mold and occupies a half of the length. By contrast, another highly complex behavior is observed in the other half of the figure, the region close to the SEN.

The structure of the liquid level fluctuations along a ten-seconds video clip is shown in Fig. 9. The 3,000 edges detected for this video clip are included in this figure. The axis without a label is the front wall of the mold, divided into 512 samples, one sample for each pixel. For clarity, the surface was not colored. It can be observed that the dynamic behavior of the liquid level height is highly complex. This figure shows again a quasi-periodic behavior in the zone near the narrow-wall of the mold.

4.2. Long-time scale

The experimental results previously presented suggest that the transient behavior of the liquid free surface has a periodic nature. This section presents a formal analysis of the power

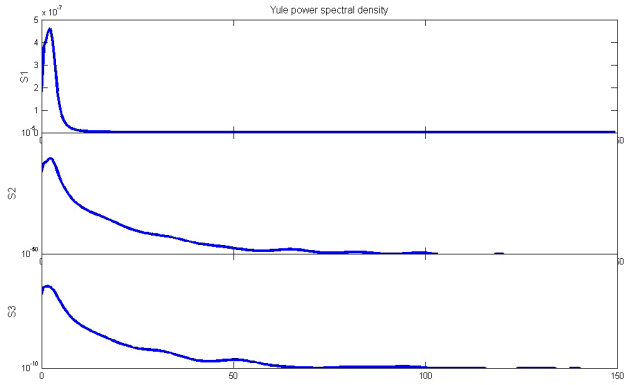

FIGURE 10. Spectral analysis with a frequency of 300 samples per second.

spectral density of the level fluctuations in order to characterize the dominant periodic components [24-25].

A power spectral density analysis of the level measurements in three selected points along the wide wall of the mold was done. These locations match with pixels 113 (S1), 227 (S2) and 340 (S3), which correspond to distances of 0.0527 m, 0.1055 m and 0.1580 m respectively. The distances are measured from the narrow-wall side towards the center of the mold.

Figure 10 shows the results of the power spectral density analysis of the signals S1, S2 and S3 from a two-minute long video clip. The Yule method, also known as auto-correlation method, was employed. The analysis shown in this figure includes the obtained results from processing 36,000 images at 300 samples per second.

Figure 10 shows that the signals were over-sampled because the fundamental frequencies are much less than 75 Hz, in accordance with the Nyquist–Shannon sampling theorem [25]. However, the over-sampling was necessary to obtain a well-defined edge of the water level.

To characterize the low frequencies components and to obtain additional information of the signals, the sampling rate must be reduced. The process of reducing a sampling rate by an integer factor is known as "down-sampling of a data sequence" [25]. To reduce the data sequence, $x(n)$, by an integer factor M, the following equation must be applied:

$$y(m) = x(nM), \tag{1}$$

where $y(m)$ is the down-sampled sequence, obtained by taking one sample of the data sequence $x(n)$ by every M samples. With this process, all the M-1 samples are discarded, in every set of M samples.

Figures 11a, 11b, and 11c show the spectrum of signals S1, S2 and S3 using sampling rates of 10.0, 1.0 and 0.5 Hz, respectively. Figure 11a shows a periodic component of the liquid level signal with a characteristic frequency close to 2.5 Hz. This value is in accordance with the results discussed in previous sub-section and that reported in previous works [8].

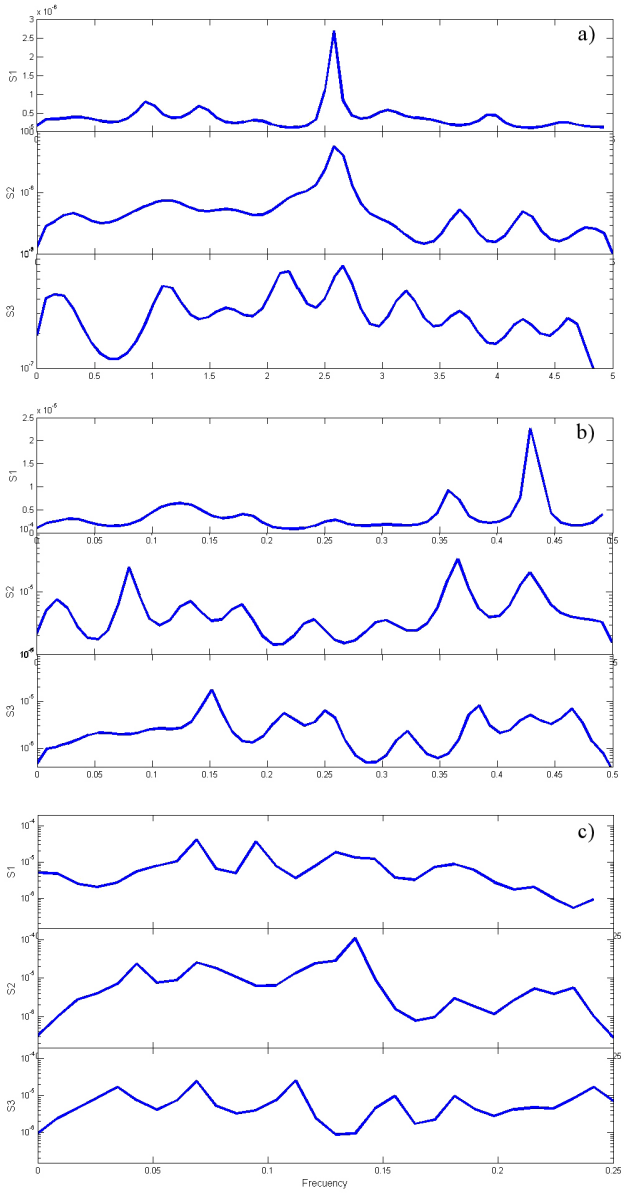

FIGURE 11. Spectral analysis of signals S1, S2 and S3 using different sampling frequencies.

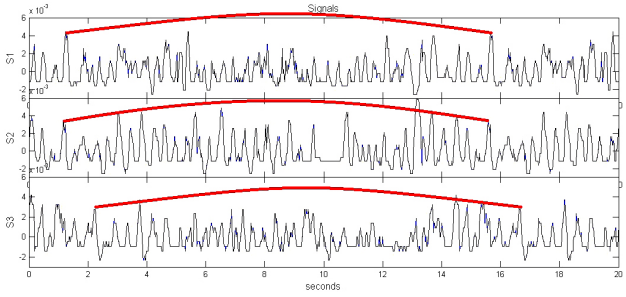

FIGURE 12. Dynamic behavior of the water levels measurements.

There are significant differences on the spectra shown in Fig. 11. Figure 11a shows a periodic behavior with only one dominant component for signals S1 and S2, which are located near the narrow-wall of the mold. On the contrary, the behavior of signal S3, which is located close to the SEN, has a complex behavior with numerous periodic components.

When the sampling rate is reduced to 1.0 Hz, there is no coincidence in any periodic component for the three signals, as shown in Fig. 11b. However, for a sampling rate of 0.5 Hz, there is a common periodic component in all the signals. The period of this component is close to 14.4 s. For this sampling rate, other frequencies were also detected; nevertheless they could be attributed to aliasing noise.

Figure 12 shows the dynamic behavior of the liquid levels at locations S1, S2 and S3 during an interval of 20 seconds long. To smooth out these signals, only partial data are presented (60 samples per second). It is clear that the liquid height signals for each location are different. Although, the three signals were taken at different points, Fig. 12 shows that each signal is replicated almost exactly each 14.4 seconds. As reference, three markers whose length is 14.4 seconds were included in this figure.

The biggest variations in the amplitude of the signals are observed in S2. The smallest variations in the amplitude of the signals are observed in S3. This behavior is in accordance with previous works, where it is reported that the zone near the SEN presents the smallest changes in the liquid level amplitude.

5. Concluding remarks

This work showed that the fluctuations and the periodicity of the liquid level inside a scaled model of the mold section of a continuous casting machine can be accurately studied by using the Sobel image-processing technique. To obtain well-defined edges, images from high-speed video clips were used in this work.

The results of the power spectra analysis showed a quite evident periodic behavior in the zone near the narrow-wall of the mold. This analysis also shows a highly complex behavior in the zone close to the SEN.

For the mold geometry and operation conditions used in the experimental simulations reported in this work, a periodic behavior with two dominant components was obtained. The periods of the components were 0.4 and 14.4 seconds. However, further studies of the relationship between the parameters of the process and the magnitude of the characteristic frequencies must be done.

The methodology proposed in this work, allows rebuilding the two-dimensional structure of the dynamic behavior of the level profile in a scaled model of the mold. Eventually, the obtained results using this methodology can be used to develop a soft-sensor of the type ”data-driven”, which could control the liquid steel level in a current continuous casting process.

Acknowledgments

The authors are grateful for the financial support to Sistema Nacional de Investigadores (SNI-CONACYT) as well as to the Universidad Autonoma Metropolitana for grants for Research Projects. The authors also wish to acknowledge the support of the Laboratorio de Computo Cientifico - Departamento de Sistemas at Universidad Autonoma Metropolitana-Azcapotzalco.

---

1. C.H. Yim, and O. Kwon, *Journal of Iron and Steel Research International* **15** (2008) 52-58.
2. C. Real, *et al.*, *ISIJ International* **46** (2006) 1183-1191.
3. B. You, *et al.*, *ISIJ International* **49** (2009) 1174-1183.
4. M.A. Barron, R. Aguilar, and J. Gonzalez, *IEEE Transactions on Industry Applications* **36** (2000) 861-864.
5. M.A. Barron, R. Aguilar, and J. Gonzalez, *IEE Proceedings-Control Theory and Applications* **147** (2000) 416-420.
6. I.K. Craig, F.R. Camisani-Calzolari, and P.C. Pistorius, *Control Engineering Practice* **9** (2001) 1013-1020.
7. L.F. Zhang, and B.G. Thomas, *ISIJ International*. **43** (2003) 271-291.
8. R. Miranda, *et al.*, *ISIJ International* **45** (2005) 1626-1635.
9. B.Z. Shen, H.F. Shen, and B.C. Liu, *Ironmaking & Steelmaking* **36** (2009) 33-38.
10. B.Z. Shen, H.F. Shen, and B.C. Liu, *ISIJ International* **47** (2007) 427-432.
11. Y.J. Jeon, H.J. Sung, and S. Lee, *Metallurgical and Materials Transactions B-Process Metallurgy and Materials Processing Science* **41** (2010) 121-130.
12. Q. Yuan, *et al.*, *Metallurgical and Materials Transactions B-Process Metallurgy and Materials Processing Science*. **35** (2004) 967-982.
13. D. Gupta, S. Chakraborty, and A.K. Lahiri, *ISIJ International* **37** (1997) 654-658.
14. D. Gupta, and A.K. Lahiri, *Metallurgical and Materials Transactions B-Process Metallurgy and Materials Processing Science*. **25** (1994) 227-233.
15. V. Singh, *et al.*, *Isij International* **46** (2006) 210-218.
16. H.F. Shen, B.Z. Shen, and B.C. Liu, *Steel Research International* **78** (2007) 531-535.
17. C. Real-Ramirez, and J. Gonzalez-Trejo, *International Journal of Minerals Metallurgy and Materials*. **18** (2011) 397-406.
18. R.C. Gonzalez, and R.E. Woods, *Digital image processing*. 3rd ed. (Upper Saddle River, N.J.: Prentice Hall. xxii, 2008) p. 954.
19. F. Arandiga, *et al.*, *Image and Vision Computing* **28** (2010) 553-562.
20. A.C. Bovik, *Academic Press series in communications, networking and multimedia* (San Diego: Academic Press. xv, 2000) p. 891.
21. T.K. Koh, *et al.*, *Minerals Engineering* **22** (2009) 537-543.
22. G. Petschnigg *et al.*, *ACM Transactions on Graphics* **23** (2004) 664-672.
23. M.S. Nixon and A.S. Aguado, *Feature extraction and image processing*. 1st ed., (Oxford ; Boston: Newnes. xii, 2002) p. 350
24. S.W. Smith, *Digital signal processing : a practical guide for engineers and scientists*. (Demystifying technology series. Amsterdam ; Boston: Newnes. xiv, 2003). p. 650
25. D.F. Elliott, *Handbook of digital signal processing : engineering applications* (San Diego: Academic Press. xxii, 1987). p. 999